New studies and predictions for nuclear clustering and dynamics in the *ab initio* symmetry-adapted framework

Kristina D. Launey[1,*], *Darin* C. Mumma[1], *Kevin* S. Becker[1], *Grigor* H. Sargsyan[2], *William* P. Good[3], *Adriana* R. Baniecki[4], *Aidan* W. Kelly[5], and *Alexis* Mercenne[1]

[1]Department of Physics and Astronomy, Louisiana State University, Baton Rouge, LA 70803, USA
[2]Facility for Rare Isotope Beams, Michigan State University, East Lansing, MI 48824, USA
[3]Department of Physics and Astronomy, Michigan State University, East Lansing, MI 48824, USA
[4]Department of Physics and Astronomy, University of Notre Dame, Notre Dame, 46556, IN, USA
[5]Eberly College of Science, Pennsylvania State University, University Park, PA 16802, USA

Abstract. We discuss recent studies and predictions for nuclear clustering and dynamics within the framework of the *ab initio* symmetry-adapted no-core shell model, which has opened new domains of the nuclear chart. In this framework, we show the emergence from first principles of collectivity and clustering in light to medium-mass nuclei, with implications for constructing *ab initio* optical potentials, for studying clustering in stable and unstable nuclei, for reproducing enhanced deformations without effective charges, and for the formation of clusters and its sensitivity to the underlying inter-nucleon force.

1 Introduction

Ab initio descriptions of spherical and deformed nuclei up through the calcium region are now possible without the use of renormalization procedures and effective charges, in the framework of the symmetry-adapted no-core shell model (SA-NCSM) [1–3]. In particular, the SA-NCSM can use significantly reduced model spaces as compared to the corresponding ultra-large conventional model spaces without compromising the accuracy of results for various observables. This allows the SA-NCSM to accommodate clustering, collective, and continuum degrees of freedom, as well as to reach heavier nuclei, such as ^{20}Ne [2], ^{21}Mg [4], ^{22}Mg [5], ^{28}Mg [6], ^{32}Ne and ^{48}Ti [3, 7], ^{40}Ca [8, 9], as well as $^{20-40}$Mg using a hybrid SA-NCSM-plus-neural-network machine learning approach [10]. A key ingredient of the SA concept is the symplectic $\mathrm{Sp}(3,\mathbb{R})\supset\mathrm{SU}(3)$ symmetry; indeed, we have found that in nuclear low-lying states, this symmetry emerges as an almost perfect symmetry from first principles [2].

Many nuclear shapes relevant to low-lying states are included in conventional shell-model spaces, however, the vibrations of deformed equilibrium shapes and spatially extended modes, such as clustering modes, often lie outside such spaces. The selected model space in the SA-NCSM remedies this, and includes those configurations in a well prescribed way. This is critical for enhanced deformation, since spherical and less deformed shapes easily develop in comparatively small model-space sizes.

In this paper, we discuss the recent developments for constructing, for the first time, translationally invariant optical potentials rooted in first principles for proton, neutron, and deuteron projectiles, applicable to stable and unstable targets up through the Ca region and at the astrophysically relevant energy regime. We also discuss the impact of α-clustering in ^{8}Be on theoretical predictions that help probe physics beyond the Standard Model through high-precision beta-decay experiments [11–13]. Interestingly, these calculations suggest low-lying 0^+ and 2^+ intruder states that are not in the experimental ^{8}Be spectrum but have been previously proposed by R-matrix fits [14, 15]. While these states appear to be very short lived and one can argue that they are not a part of the ^{8}Be physics, Refs. [12, 16–18] have shown that including these in the theory can significantly affect nuclear observables, such as Gamow-Teller (GT) transition strengths. Furthermore, we discuss the challenging α+^{12}C substructure in low-lying states of ^{16}O, which, in turn, provide the first local α+^{12}C effective interaction with uncertainties that fully reflect the microscopic content of the clusters and can be used in many current few-body reaction codes. In addition, we briefly outline an extension of the theory to unstable proton-rich oxygen isotopes, including p+^{14}O and the interesting α-capture reaction on ^{15}O with implications to x-ray burst nucleosynthesis. These applications build upon the successful *ab initio* symmetry-adapted no-core shell model that has expanded the reach of practically exact methods to medium-mass open-shell nuclei.

2 *Ab initio* optical potentials

In many-body approaches, the complexity of the problem grows exponentially with the number of particles and the space in which they reside. A more general approach to reactions that is especially suitable for heavier nuclei is

*e-mail: klauney@lsu.edu

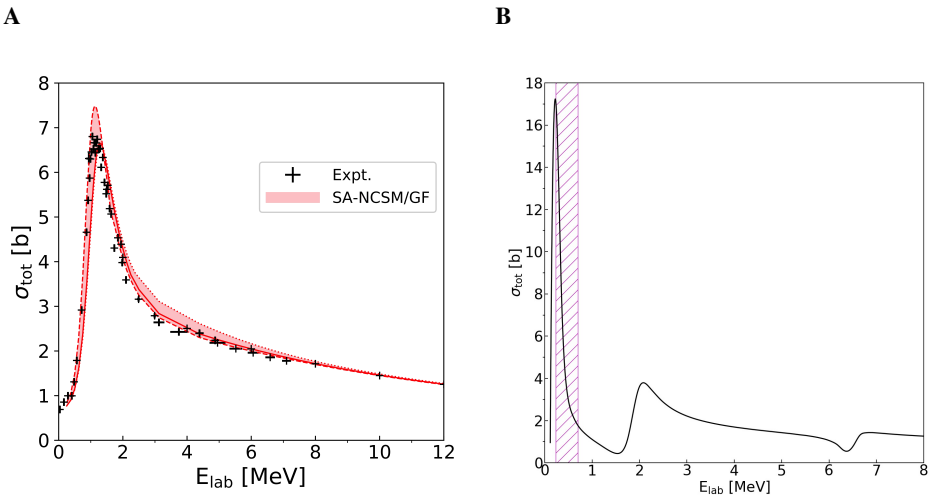

Figure 1. Calculated total cross sections vs. laboratory-frame projectile kinetic energy using the *ab initio* SA-NCSM/GF for two cases. **A**. Plot of n+^{4}He across $\hbar\Omega$ = 12 (red dashed), 16 (red solid), and 20 MeV (red dotted) compared to three sets of experimental data [19–21] (labeled as "Expt."). The red band shows the $\hbar\Omega$ = 12-20 MeV spread, to guide the eye. Figure adapted from [22]. **B.** Plot of n+^{6}He for $\hbar\Omega$ = 12 MeV (black solid) compared to the experimental energy of the $^2P_{3/2}$ resonance with its uncertainty (vertical hashed bar). Figure adapted from [23].

based on identifying few-body degrees of freedom, typically the reaction fragments (or clusters) involved in the reaction, and reducing the many-body problem to a few-body technique [24]. As this reduction results in effective interactions (often referred to as "optical potentials") between the clusters, the need for parameter-free interactions has been recognized especially away from stability, where uncertainties become uncontrolled, since elastic scattering data does not fully constrain the optical potential [25].

To address this, recent studies have utilized realistic inter-nucleon interactions, typically derived in the chiral effective field theory, without the need to fit interaction parameters in the nuclear medium. These models have built upon earlier theoretical frameworks, such as the Green's function technique [26] and the dispersive optical model [27–29], as well as the spectator expansion of the multiple scattering theory for elastic scattering of a single-nucleon projectile [30–32]. Recent applications include *ab initio* nucleon-nucleus potentials for elastic scattering for closed-shell nuclei at low projectile energies ($\lesssim$ 20 MeV per nucleon) based on the Green's function technique with the coupled-cluster method [33, 34] and the self-consistent Green's function method [35], as well as the spectator expansion of the multiple scattering theory in the intermediate-energy regime ($\gtrsim$ 100 MeV per nucleon) [36, 37] (see also Ref. [38]). Similarly, optical potentials have been derived from two- and three-nucleon chiral forces in nuclear matter [39]. These potentials provide cross sections for elastic proton or neutron scattering and additionally can be used as input to modeling (d,p) and (d,n) reactions [40].

We have recently constructed *ab initio* nucleon-nucleus (NA) optical potentials that are fully translationally invariant and applicable to a broad range of open-shell spherical and deformed nuclei. We achieve this by combining the Green's function (GF) approach with the SA-NCSM [2, 3]. In addition, an important advantage of the GF technique is that the NA effective potentials include the information about all near-reaction channels through the GF calculations in the ($A \pm 1$) systems. In this SA-NCSM/GF framework, we illustrate the new developments for the elastic neutron scattering off the ^{4}He ground state, as well as the ^{6}He ground state [22]. We show that phase shifts and cross sections agree remarkably well with experimental values (see figure 1 for cross sections).

An important feature of the SA-NCSM/GF optical potentials is that they exactly treat the center-of-mass motion, and hence, are translationally invariant. Another important feature is that collective excitations are readily available in the SA-NCSM framework. Indeed, missing collective correlations have been suggested to reduce absorption in scattering at lower energies [33]. Hence, this study opens the path for exploring proton and neutron scattering on intermediate- and medium-mass targets, including the role of collectivity and clustering.

3 Alpha-clustering from first principles

Earlier *ab initio* SA-NCSM studies have shown that alpha clustering naturally emerges from the underlying chiral potentials [2, 3]. Indeed, the SA-NCSM framework is ideal to explore surface clustering, as done in Refs. [12, 41, 43]. Ref. [43] has recently presented a new many-body technique for calculating α spectroscopic amplitudes, as well as for determining challenging α widths and asymptotic normalization coefficients (ANCs) utilizing *ab initio* SA-NCSM wave functions, with a focus on the ^{16}O(α,γ)^{20}Ne reaction rate. Indeed, the SA framework is ideal for addressing cluster substructures, as it enables large model spaces needed for clustering, and capitalizes

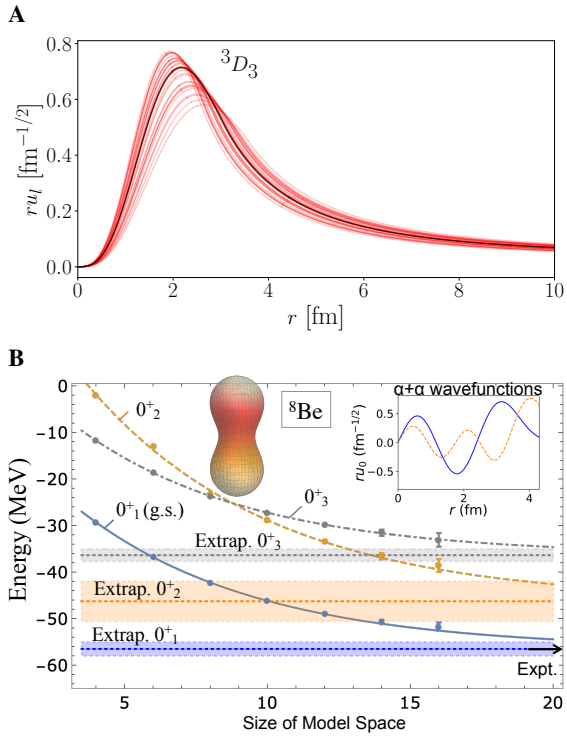

Figure 2. **A.** $\alpha + d\ ^3D_3$ partial waves for the 3^+ resonance of ^{6}Li as functions of the cluster separation r, obtained from *ab initio* SA-NCSM wave functions computed with the NNLO$_{\rm opt}$ chiral potential (black) and the 32 LEC parameterizations discussed in the text (red). Figure adapted from [41]. **B.** Calculated ^{8}Be low-lying 0^+ state energies illustrated for the NNLOopt chiral potential vs. the model-space size (up to 18 harmonic oscillator shells or $N_{\rm max} = 16$), together with the extrapolated values (dotted lines) and uncertainties (bands), compared to the measured $0^+_{\rm g.s.}$ energy [42] (black arrow). Inset: α+α S partial wave for $0^+_{\rm g.s.}$ (blue solid) and 0^+_2 (orange dashed). Figure adapted from [12].

on the complementary nature of the symplectic basis and the cluster basis [44–46]. Several studies have taken advantage of that relationship using a single SU(3) deformation for the clusters. For example, this approach has been used to describe the sub-Coulomb ^{12}C+^{12}C resonances of ^{24}Mg [47] of particular interest in astrophysics, as well as spectroscopic factors for α-conjugate nuclei (that is, nuclei with multiples of two protons and two neutrons) [45, 46, 48]. These studies have shown that the most important shell-model configurations can be realized by excitations of the relative motion of the two clusters.

We follow the procedure outlined in Ref. [43] to calculate α spectroscopic amplitudes (or α-cluster wave functions) and to analyze the impact of uncertainties in the underlying nucleon-nucleon (NN) force on α clustering in light nuclei. We focus on the first excited 3^+ state of ^{6}Li (figure 2**A**), which is a low-lying resonance at 0.7117 MeV above the α-d threshold [49]. We utilize the SA-NCSM wave functions for the 3^+ state, as detailed in [41]. The state is comprised of thirteen highly dominant shapes, in addition to all configurations with 0 and 2 harmonic oscillator (HO) quanta above the valence level, up to 10 HO shells. We simultaneously vary all 14 NNLO parameters, the so-called low-energy constants (LECs), within ±10% of the corresponding NNLO$_{\rm opt}$ parameterization [50], and uniformly draw 32 LEC combinations following a Latin hypercube design [51]. By doing so, Ref. [41] has shown that the properties of the α-d D partial wave $ru_{\ell=2}(r)$ for the first 3^+ in ^{6}Li significantly depend on the underlying chiral potential. Namely, as evident from figure 2**A**, 10% variations affect not only the tail, which informs how spatially extended the resonance is, but also impact the magnitude of the peak and its location (inter-cluster distance r), which describe the surface α clustering [41, 52].

Large-scale calculations of the ^{8}Be energy spectrum and long-range observables are extremely challenging, but become feasible in the SA-NCSM framework (figure 2b). Refs. [11–13] have recently reported the first *ab initio* calculations of higher-order terms, the so-called recoil-order terms, in the β decays of ^{8}Li and ^{8}B to ^{8}Be, for which accurate wave functions of ^{8}Li, ^{8}B, and ^{8}Be are computed in the SA-NCSM (see figure 2**B** for low-lying 0^+ states of ^{8}Be). The recoil-order form factors are generally neglected in beta-decay theory since they are of the order of q/m_N or higher, where q is the momentum transfer and m_N is the nucleon mass. For most beta decays, the recoil effects are typically less than a percent of the dominant Fermi and GT contributions. However, for measurements of sufficiently high precision, these terms must be included in the analysis especially when the leading contributions are suppressed or the recoil-order terms are unusually large, as in the case of the ^{8}Li and ^{8}B beta decays. The calculations of Ref. [12] achieve highly reduced uncertainties compared to the experimentally extracted values of [54], largely due to an important correlation found between long-range recoil-order form factors and the quadrupole moment of the ^{8}Li (and ^{8}B) ground state. These theoretical predictions have helped high-precision experiments to decrease the systematic uncertainties and place the most stringent limit on the tensor-current estimates in the weak interaction as reported in Refs. [11, 13]. In addition, these calculations are of interest to experimental tests of the conserved vector current hypothesis [55].

Remarkably, the ^{8}Be calculations in unprecedentedly large model spaces of Ref. [12] support the existence of low-lying 0^+_2 and 2^+_2 states in the ^{8}Be spectrum (sometimes referred to as "intruder" states) exhibiting a large overlap with the $\alpha + \alpha$ S and D partial waves, respectively (see figure 2**B** for the 0^+_2). Namely, the infinite-space extrapolations determine the energies of the 0^+_2 and 2^+_2 between 5 and 15 MeV above the ground state. Indeed, a very broad 2^+ state and a lower 0^+ state were initially proposed by Barker from the R-matrix analysis of $\alpha + \alpha$ scattering and the β decays of ^{8}Li and ^{8}B [14, 15, 17]. Even though such states have not been directly observed experimentally, there have been experimental indications [56] and theoretical predictions in favor of intruder states below 16 MeV [57–59]. In addition, the SA-NCSM calculations yield α partial widths that are in good agreement with

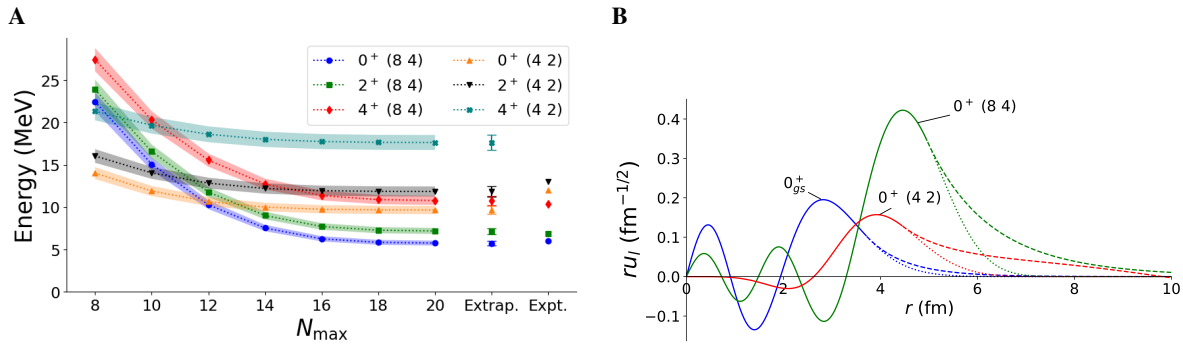

Figure 3. **A.** Excitation energies of low-lying states in ^{16}O, labeled by the $(\lambda\,\mu)$ SU(3) quantum numbers of their dominant equilibrium deformation, as functions of the model space size or $N_{\max}$. Error bars are from 5% variations of the harmonic oscillator frequency. Also shown are the infinite-size limits (labeled as "Extrap."), which are compared to experiments where available (labeled as "Expt."). Note that the size of the $N_{\max} = 14$ complete model space is 5.4×10^{12}, which is currently inaccessible but becomes feasible as far as $N_{\max} = 20$ within the NCSpM framework. **B.** α+^{12}C S partial waves, $ru_{\ell=0}(r)$, for the lowest three 0^+ states in ^{16}O, where the interior region is determined by the many-body descriptions of the states and is matched in an R-matrix approach to the asymptotic behavior given by the exact Coulomb eigenfunction. Figures adapted from [53].

experimentally deduced values [60]. For example, the α width for the 0^+ ground state is estimated to be 5.7 eV, compared with 5.57 eV [60], and for the 2^+_1 state the SA estimate is 1.3 MeV, compared to 1.5 MeV.For the intruder states, the SA estimates are 10(2) MeV and 10(3) MeV for the 0^+_2 and 2^+_2 states, respectively. We note that except for the $0^+_{\text{g.s.}}$ width that uses the experimental threshold of -92 keV relative to the ^{8}Be ground state, all the widths use the α+α threshold estimated at -104 keV from the SA-NCSM extrapolations of the ^{4}He and ^{8}Be binding energies with NNLO$_{\text{opt}}$. The very large α widths of the intruder states suggest that these states are extremely short lived, and one may argue that they should not be considered as a part of the ^{8}Be spectrum. Nonetheless, Refs. [13, 18] have also provided evidence that the intruder 2^+_2 state significantly affects the β-transition strength of the ^{8}Li and ^{8}B decays, and thus this state becomes important for accurate theoretical predictions.

Within this framework, it is interesting to explore the α-capture reaction on ^{15}O [23] with implications to x-ray burst nucleosynthesis. In particular, we determine the α partial width for the $3/2^+$ in ^{19}Ne, which has been the focus of past experimental efforts as well as planned experiments at rare isotope beam facilities. To achieve this, the $3/2^+$ state in ^{19}Ne is calculated in the *ab initio* SA-NCSM with the NNLO$_{\text{opt}}$ chiral potential in 15 HO shells. This yields a partial α width of $\Gamma_\alpha = 5.66\times10^{-6}$ eV [23], which corroborates the outcomes of earlier measurements.

4 α+^{12}C and toward α-nucleus optical potentials

We examine alpha-clustering in low-lying states of ^{16}O [53] within a microscopic approach based on the no-core symplectic shell model (NCSpM) [61], successfully applied earlier to the Hoyle state in ^{12}C. According to the symplectic symmetry, found through SA-NCSM calculations to naturally emerge from first principles and to be an almost perfect symmetry in nuclei [2], we consider the most dominant shapes for these states. Each of these shapes is labeled by its equilibrium deformation, an SU(3) $(\lambda\,\mu)$ configuration [we remind that $(0\,0)$, $(\lambda\,0)$, and $(0\,\mu)$ describe spherical, prolate, and oblate deformation, respectively]. Hence, for the ground state, we use a $(0\,0)$ symplectic subspace: this describes a spherical 0-particle-0-hole (0p-0h) equilibrium deformation, along with its prolate vibrations up through 22 HO shells ($N_{\max} = 20$). We find that the next 0^+_2 state in the energy spectrum of ^{16}O is described by a highly deformed 4p-4h configuration, $(8\,4)$, whereas a 2p-2h $(4\,2)$ configuration lies higher in energy (figure 3**A**). The α+^{12}C S-waves for these 0^+ states suggest that they exhibit different clustering behavior (figure 3**B**). Namely, the large peak around 4.5 fm for the 0^+_2 demonstrates strong surface clustering in the excited 0^+_2 state that is not seen in the tightly bound ground state, which instead shows several peaks of similar magnitude. This means that in the ground state, the α clusters highly overlap, while the other two 0^+ states show a high probability for α-cluster formation on the surface.

These α+^{12}C cluster wave functions are, in turn, used to deduce a local effective cluster interaction [62] that can be readily utilized in many current reaction codes. To do so, we employ Bayesian analysis that adopts a Gaussian likelihood function. This likelihood function minimizes the differences between the microscopic α+^{12}C cluster wave functions and those computed from an effective Woods-Saxon interaction with two parameters for two point-particles, normalized to the microscopically calculated spectroscopic factor (which is the norm of the microscopic α+^{12}C cluster wave functions).

For the Bayesian fitting procedure, the radius of the potential well is fixed at $R = 2.40$ fm. We utilize a Markov chain Monte Carlo algorithm with walkers that explore the parameter space with uniform prior distributions for the potential depth V in the interval $[-110, -80]$ MeV and diffusion a in the interval $[0.4, 0.7]$ fm. The

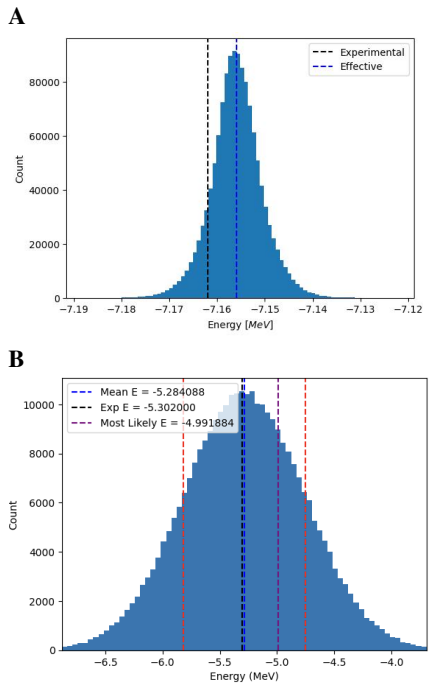

Figure 4. A. Posterior energy distribution of the α+^{12}C S-wave, with the mean of the distribution (blue) and the experimentally measured value (black) indicated. Figure adapted from [62]. **B.** Posterior energy distribution of the p+^{14}O S-wave, with the result obtained by maximizing the likelihood function (purple), the mean value (blue) and 1σ interval (red) of the distribution, and the experimentally measured value (black) indicated. Figure adapted from [63].

procedure provides probability density functions of the V and a parameters that are very close to Gaussian distributions with centroids and standard deviations as follows: $V = -91.64 \pm 0.01$ MeV and $a = 0.450 \pm 0.004$ fm. The probability density functions for the Woods-Saxon parameters provide, in turn, probability density functions for various structure and reaction observables. For example, the energy distribution for the ^{16}O ground state yields a mean that is only 6 keV away from the experimental value (figure 4**A**) [62].

Similarly, this procedure can be extended to unstable nuclei, with the goal to provide reliable cluster potentials with uncertainties in the region where experimental measurements are not available or are sparse. For example, a recently deduced p+^{14}O cluster interaction with uncertainties [63] yields energy distribution for the lowest-energy resonance $\frac{1}{2}^+$ in ^{15}F that closely agrees with the experimental value, as illustrated in figure 4**B**, and is much broader, compared to that of the tightly bound ground state of ^{16}O.

5 Conclusions

We discuss several applications of the symmetry-adapted framework. We show that the use of the SA basis is essential, first, for structure observables, especially for precise descriptions of cluster formation in nuclei and of collectivity in medium-mass nuclei. Second, the SA basis enables couplings to the continuum, through excitations that are otherwise inaccessible. This is critical to calculating reaction observables and deriving nucleon- and α-nucleus potentials rooted in first principles for low energies, which coincides with the astrophysically relevant regime. As these approaches build upon first principles, we show that clustering features are sensitive to the parameterization of the underlying NN interaction and can be used as probes to further constrain these interactions.

In short, with the help of high-performance computing resources, the use of the SA concept in *ab initio* studies represents a powerful tool to tackle structure and reactions of nuclei, and it is manageable as well as expandable, while utilizing at each stage the predictive power of the *ab initio* approach.

Acknowledgements

We acknowledge the support from the U.S. National Science Foundation (PHY-2209060) as well as from its REU site in Physics & Astronomy at Louisiana State University (NSF Grant No. 2150445), and the U.S. Department of Energy (DE-SC0023532, & under the FRIB Theory Alliance award DE-SC0013617). This work benefited from high performance computational resources provided by LSU, NERSC, and the Frontera computing project.

References

[1] K.D. Launey, T. Dytrych, J.P. Draayer, Symmetry-guided large-scale shell-model theory, Prog. Part. Nucl. Phys. **89**, 101 (review) (2016). 10.1016/j.ppnp.2016.02.001

[2] T. Dytrych, K.D. Launey, J.P. Draayer, D.J. Rowe, J.L. Wood, G. Rosensteel, C. Bahri, D. Langr, R.B. Baker, Physics of nuclei: Key role of an emergent symmetry, Phys. Rev. Lett. **124**, 042501 (2020). 10.1103/PhysRevLett.124.042501

[3] K.D. Launey, A. Mercenne, T. Dytrych, Nuclear dynamics and reactions in the ab initio symmetry-adapted framework, Annu. Rev. Nucl. Part. Sci. **71**, 253 (2021). 10.1146/annurev-nucl-102419-033316

[4] P. Ruotsalainen, J. Henderson, G. Hackman, G.H. Sargsyan, K.D. Launey et al., Isospin symmetry in $B(E2)$ values: Coulomb excitation study of ^{21}Mg, Phys. Rev. C **99**, 051301 (2019). 10.1103/PhysRevC.99.051301

[5] J. Henderson et al., Testing microscopically derived descriptions of nuclear collectivity: Coulomb excitation of ^{22}Mg, Phys. Lett. **B782**, 468 (2018). 10.1016/j.physletb.2018.05.064

[6] J. Williams, G.C. Ball, A. Chester et al., Structure of ^{28}Mg and influence of the neutron pf shell, Phys. Rev. C **100**, 014322 (2019). 10.1103/PhysRevC.100.014322

[7] K.D. Launey, A. Mercenne, G.H. Sargsyan, H. Shows, R.B. Baker, M.E. Miora, T. Dytrych,

J.P. Draayer, Emergent clustering phenomena in the framework of the *ab initio* symmetry-adapted no-core shell model, in *Proceedings of SOTANCP4, May 2018, Galveston, Texas* (AIP Conference Proceedings, 2018), Vol. 2038, p. 020004, https://doi.org/10.1063/1.5078823

[8] M. Burrows et al., Response functions and giant monopole resonances for light to medium-mass nuclei from the *ab initio* symmetry-adapted no-core shell model, arXiv:2312.09782 (2024). 10.48550/arXiv.2312.09782

[9] R.B. Baker, C. Elster, T. Dytrych, K.D. Launey, Ab initio leading order effective potential for elastic proton scattering based on the symmetry-adapted no-core shell model, Phys. Rev. C **110**, 034605 (2024). 10.1103/PhysRevC.110.034605

[10] O.M. Molchanov, K.D. Launey, A. Mercenne, G.H. Sargsyan, T. Dytrych, J.P. Draayer, Machine learning approach to pattern recognition in nuclear dynamics from the ab initio symmetry-adapted no-core shell model, Phys. Rev. C **105**, 034306 (2022). 10.1103/PhysRevC.105.034306

[11] M.T. Burkey, G. Savard, A.T. Gallant, N.D. Scielzo, J.A. Clark, T.Y. Hirsh, L. Varriano, G.H. Sargsyan, K.D. Launey et al., Improved limit on tensor currents in the weak interaction from ^{8}Li β decay, Phys. Rev. Lett. **128**, 202502 (2022). 10.1103/PhysRevLett.128.202502

[12] G.H. Sargsyan, K.D. Launey, M.T. Burkey, A.T. Gallant, N.D. Scielzo, G. Savard, A. Mercenne, T. Dytrych, D. Langr et al., Impact of clustering on the ^{8}Li β decay and recoil form factors, Phys. Rev. Lett. **128**, 202503 (2022). 10.1103/PhysRevLett.128.202503

[13] B. Longfellow, A.T. Gallant, G.H. Sargsyan et al., Improved tensor current limit from ^{8}B β decay including new recoil-order calculations, Phys. Rev. Lett. **132**, 142502 (2024). 10.1103/PhysRevLett.132.142502

[14] F. Barker, H. Hay, P. Treacy, 0^{+} states of ^{8}Be, Aust. J. Phys. **21**, 239 (1968). 10.1071/PH680239

[15] F. Barker, 2^{+} states of ^{8}Be, Aust. J. Phys. **22**, 293 (1969). 10.1071/PH690293

[16] E.K. Warburton, R-matrix analysis of the $\beta^{\mp}$-delayed alpha spectra from the decay of ^{8}Li and ^{8}B, Phys. Rev. C **33**, 303 (1986). 10.1103/PhysRevC.33.303

[17] F. Barker, Delayed alpha spectra from the beta decay of ^{8}Li and ^{8}B, Aust. J. Phys. **42**, 25 (1989). 10.1071/PH890025

[18] S. Hyldegaard, Ph.D. thesis, Aarhus University (2010), http://phys.au.dk/fileadmin/site_files/publikationer/phd/Solveig_Hyldegaard.pdf

[19] B. Haesner, W. Heeringa, H.O. Klages et al., Measurement of the ^{3}He and ^{4}He total neutron cross sections up to 40 MeV, Phys. Rev. C **28**, 995 (1983). 10.1103/PhysRevC.28.995

[20] J.H. Coon, Total neutron cross sections of the hydrogen and helium isotopes, Nuclear Physics **12**, 291 (1959). 10.1016/0029-5582(59)90175-0

[21] S. Bashkin, F.P. Mooring, B. Petree, Total cross section of helium for fast neutrons, Phys. Rev. **82**, 378 (1951). 10.1103/PhysRev.82.378

[22] M. Burrows, K.D. Launey, A. Mercenne, R.B. Baker, G.H. Sargsyan, T. Dytrych, D. Langr, Ab initio translationally invariant nucleon-nucleus optical potentials, Phys. Rev. C **109**, 014616 (2024). 10.1103/PhysRevC.109.014616

[23] D.C. Mumma et al., Astrophysically important alpha capture reaction on ^{15}O from *ab initio* calculations of ^{19}Ne, (to be submitted) (2024).

[24] I.J. Thompson, F.M. Nunes, Nuclear Reactions for Astrophysics: Principles, Calculation and Applications of Low-Energy Reactions (Cambridge University Press, 2009), https://doi.org/10.1017/CBO9781139152150

[25] A. Lovell, F. Nunes, Systematic uncertainties in direct reaction theories, J. Phys. G **42**, 034014 (2015). 10.1088/0954-3899/42/3/034014

[26] F. Capuzzi, C. Mahaux, Relationship between Feshbach's and Green's function theories of the nucleon–nucleus mean field, Annals of Physics **281**, 223 (2000). 10.1006/aphy.2000.6011

[27] C. Mahaux, H. Ngo, G.R. Satchler, Causality and the threshold anomaly of the nucleus-nucleus potential, Nucl. Phys. A **449**, 354 (1986). 10.1016/0375-9474(86)90009-6

[28] C. Mahaux, R. Sartor, Single-Particle Motion in Nuclei (Springer US, Boston, MA, 1991), pp. 1–223, ISBN 978-1-4613-9910-0, https://doi.org/10.1007/978-1-4613-9910-0_1

[29] W.H. Dickhoff, D. Van Neck, Many-Body Theory Exposed!, 2nd edn. (WORLD SCIENTIFIC, 2008), https://www.worldscientific.com/doi/abs/10.1142/6821

[30] K.M. Watson, Multiple scattering and the many-body problem—applications to photomeson production in complex nuclei, Phys. Rev. **89**, 575 (1953). 10.1103/PhysRev.89.575

[31] A.K. Kerman, H. McManus, R.M. Thaler, The scattering of fast nucleons from nuclei, Ann. Phys. **8**, 551 (1959). 10.1016/0003-4916(59)90076-4

[32] E.R. Siciliano, R.M. Thaler, Spectator expansion in multiple scattering theory, Phys. Rev. C **16**, 1322 (1977). 10.1103/PhysRevC.16.1322

[33] J. Rotureau, P. Danielewicz, G. Hagen, F.M. Nunes, T. Papenbrock, Optical potential from first principles, Phys. Rev. C **95**, 024315 (2017). 10.1103/PhysRevC.95.024315

[34] J. Rotureau, P. Danielewicz, G. Hagen, G.R. Jansen, F.M. Nunes, Microscopic optical potentials for calcium isotopes, Phys. Rev. C **98**, 044625 (2018). 10.1103/PhysRevC.98.044625

[35] A. Idini, C. Barbieri, P. Navrátil, Ab initio optical potentials and nucleon scattering on medium

mass nuclei, Phys. Rev. Lett. **123**, 092501 (2019). 10.1103/PhysRevLett.123.092501

[36] M. Burrows, R.B. Baker, C. Elster, S.P. Weppner, K.D. Launey, P. Maris, G. Popa, Ab initio leading order effective potentials for elastic nucleon-nucleus scattering, Phys. Rev. C **102**, 034606 (2020). 10.1103/PhysRevC.102.034606

[37] M. Vorabbi, M. Gennari, P. Finelli, C. Giusti, P. Navrátil, R. Machleidt, Elastic proton scattering off nonzero spin nuclei, Phys. Rev. C **105**, 014621 (2022). 10.1103/PhysRevC.105.014621

[38] C.W. Johnson, K.D. Launey et al., From bound states to the continuum, J. Phys. G **47**, 23001 (2020), arXiv:1912.00451. 10.1088/1361-6471/abb129

[39] T.R. Whitehead, Y. Lim, J.W. Holt, Proton elastic scattering on calcium isotopes from chiral nuclear optical potentials, Phys. Rev. C **100**, 014601 (2019). 10.1103/PhysRevC.100.014601

[40] J. Rotureau, G. Potel, W. Li, F.M. Nunes, Merging ab initio theory and few-body approach for (d, p) reactions, J. Phys. G: Nucl. Part. Phys. **47**, 065103 (2020). 10.1088/1361-6471/ab8530

[41] K.S. Becker, K.D. Launey, A. Ekstrom, T. Dytrych, Ab initio symmetry-adapted emulator for studying emergent collectivity and clustering in nuclei, Front. Phys. **11**, 1064601 (2023). 10.3389/fphy.2023.1064601

[42] W. Huang, M. Wang, F. Kondev, G. Audi, S. Naimi, The AME 2020 atomic mass evaluation (I). Evaluation of input data, and adjustment procedures, Chin. Phys. C **45**, 030002 (2021). 10.1088/1674-1137/abddb0

[43] A.C. Dreyfuss, K.D. Launey, J.E. Escher, G.H. Sargsyan, R.B. Baker, T. Dytrych, J.P. Draayer, Clustering and α-capture reaction rate from ab initio symmetry-adapted descriptions of ^{20}Ne, Phys. Rev. C **102**, 044608 (2020). 10.1103/PhysRevC.102.044608

[44] K.T. Hecht, W. Zahn, An SU(3) approach to nuclear multi-cluster problems, Nucl. Phys. A **318**, 1 (1979). 10.1016/0375-9474(79)90465-2

[45] Y. Suzuki, Cluster and Symplectic Excitations in Nuclei, Nucl. Phys. A **448**, 395 (1986). 10.1016/0375-9474(86)90335-0

[46] Y. Suzuki, K.T. Hecht, Symplectic and Cluster Excitations in Nuclei: Evaluation of interaction matrix elements, Nucl. Phys. A **455**, 315 (1986). 10.1016/0375-9474(86)90021-7

[47] Y. Suzuki, K.T. Hecht, The sub-Coulomb ^{12}C+^{12}C resonances in a microscopic ^{12}C+^{12}C, α+^{20}Ne, ^{8}Be+^{16}O cluster basis, Nucl. Phys. A **388**, 102 (1982). 10.1016/0375-9474(82)90511-5

[48] K.T. Hecht, E.J. Reske, T.H. Seligman, W. Zahn, Spectroscopic amplitudes for complex cluster systems, Nucl. Phys. A **356**, 146 (1981). 10.1016/0375-9474(81)90123-8

[49] D. Tilley, C. Cheves, J. Godwin et al., Energy levels of light nuclei A=5, 6, 7, Nuclear Physics A **708**, 3 (2002). 10.1016/S0375-9474(02)00597-3

[50] A. Ekström, G. Baardsen, C. Forssén et al., An optimized chiral nucleon-nucleon interaction at next-to-next-to-leading order, Phys. Rev. Lett. **110**, 192502 (2013). 10.1103/PhysRevLett.110.192502

[51] M.D. Mckay, R.J. Beckman, W.J. Conover, A comparison of three methods for selecting values of input variables in the analysis of output from a computer code, Technometrics **42**, 55 (2000). 10.1080/00401706.2000.10485979

[52] K.S. Becker, A.R. Baniecki, A.W. Kelly, K.D. Launey, S.T. Marley, A. Mercenne, T. Dytrych, J.P. Draayer, Quantifying uncertainties in α-nucleus reaction dynamics informed from first principles, Nucl. Phys. A, in preparation (2024).

[53] W.P. Good et al., Microscopic description of the ^{12}C+alpha clustering in shape-coexisting states of ^{16}O, (to be submitted) (2024).

[54] T. Sumikama, K. Matsuta, T. Nagatomo et al., Test of the conserved vector current hypothesis by a β-ray angular distribution measurement in the mass-8 system, Phys. Rev. C **83**, 065501 (2011). 10.1103/PhysRevC.83.065501

[55] L. De Braeckeleer, E.G. Adelberger, Gundlach et al., Radiative decays of the 16.6 and 16.9 MeV states in ^{8}Be and tests of the conservation of the vector current in the A=8 multiplet, Phys. Rev. C **51**, 2778 (1995). 10.1103/PhysRevC.51.2778

[56] M. Munch, O. Sølund Kirsebom, J.A. Swartz, K. Riisager, H.O.U. Fynbo, Measurement of the full excitation spectrum of the ^{7}Li(p,γ)$\alpha\alpha$ reaction at 441 keV, Phys. Lett. B **782**, 779 (2018). 10.1016/j.physletb.2018.06.013

[57] E. Caurier, P. Navrátil, W.E. Ormand, J.P. Vary, Intruder states in ^{8}Be, Phys. Rev. C **64**, 051301(R) (2001). 10.1103/PhysRevC.64.051301

[58] P. Maris, Ab initio calculations for Be-isotopes with JISP16, in *J. Phys. Conf. Ser.* (IOP Publishing, 2013), Vol. 445, p. 012035, https://doi.org/10.1088/1742-6596/445/1/012035

[59] D. Rodkin, Y.M. Tchuvil'sky, Description of alpha-clustering of ^{8}Be nucleus states in high-precision theoretical approach, Chin. Phys. C **44**, 124105 (2020). 10.1088/1674-1137/abb4d4

[60] D. Tilley, J. Kelley, J. Godwin et al., Energy levels of light nuclei A=8,9,10, Nucl. Phys. A **745**, 155 (2004). 10.1016/j.nuclphysa.2004.09.059

[61] A.C. Dreyfuss, K.D. Launey, T. Dytrych, J.P. Draayer, C. Bahri, Hoyle state and rotational features in Carbon-12 within a no-core shell model framework, Phys. Lett. B **727**, 511 (2013). 10.1016/j.physletb.2013.10.048

[62] A.R. Baniecki et al., Alpha-^{12}C effective cluster potential with uncertainties from the many-body dynamics of ^{16}O, (to be submitted) (2024).

[63] A.W. Kelly et al., Bayesian uncertainty quantification in nuclear reaction theory for astrophysical applications, (to be submitted) (2024).